International Journal of Materials Chemistry and Physics
Vol. 1, No. 2, 2015, pp. 141-145
http://www.aiscience.org/journal/ijmcp

Fe_3O_4 Ferrofluid Nanoparticles: Synthesis and Rheological Behavior

Jyoti Dhumal, Sushilkumar Bandgar, Kisan Zipare, Guruling Shahane*

Department of Electronics, DBF Dayanand College of Arts & Science, Solapur, Maharashtra, India

Abstract

Nanocrystalline Fe_3O_4 particles of controlled size were synthesized by a facile chemical co-precipitation method. The X-ray diffraction patterns confirm the synthesis of single crystalline phase of Fe_3O_4 nanoparticles with lattice parameter 8.4090 Å. The average particle size of as-synthesized sample is 11.5 nm. A TEM analysis show that the sample contains well dispersed nanoparticles of almost spherical in shape with average particle size is of the order of 10-20 nm. The magnetic measurements show superparamagnetic nature of the sample. The saturation magnetization is 63emu/g. The rheological study of oleic acid coated Fe_3O_4 ferrofluid show magneto-viscous effect. In the absence of the magnetic field, the ferrofluids behave essentially as a Newtonian fluid having a rate-insensitive viscosity whereas increase in the magnetic field leads to strong changes in the viscosity. This can be attributed to the formation of chain-like clusters due to strong inter-particle interaction in the presence of a magnetic field.

Keywords

Fe_3O_4 Nanoparticles, Structural Characterization, Magnetic Properties, Ferrofluid

Received: August 3, 2015 / Accepted: August 12, 2015 / Published online: August 19, 2015

1. Introduction

Ferrofluid is a colloidal suspension of magnetic nanoparticles in a suitable carrier liquid, either aqueous or non-aqueous. Because of its specific characteristics, the ferrofluid behaves as a functional fluid and has found many useful applications such as dynamic sealing, dampers, heat conductors, temperature and magnetic field sensors, magnetically deformable mirrors, magnetic valve controls, fluid transformers, contrast agent for magnetic resonance imaging, DNA detection magnetic drug targeting and cancer hyperthermia treatment [1-6]. Recently, ferrofluid has been utilized in conjunction with microcontact printing to fabricate patterned structures of magnetic materials on the micron scale [7]. As each of these applications requires adapted fluid properties, it is important to develop versatile synthetic methods for ferrofluid production. There are two major steps in synthesizing a ferrofluid. The first is to make the magnetic nanoparticles (~10 nm diameter) that will be dispersed in the colloidal suspension. The second step is the dispersion of the magnetic particles into a carrier liquid by utilizing a surfactant to create a colloidal suspension. Several preparation methods are used for the synthesis of magnetic nanoparticles. These include sol-gel, hydrothermal, microwave refluxing, chemical co-precipitation, sonochemical reactions and ball milling [8-12]. Among the various methods, chemical co-precipitation method offers a low-temperature alternative to conventional powder synthesis techniques [13, 14].

One of the interesting and important features of ferrofluid is its ability to change rheological properties under the action of external magnetic field -the magneto-viscous effect [15]. Such fluids show non-Newtonian effects in presence of magnetic field. In different applications, the key parameters that dominate the process performance are viscosity and thermal conductivity of the ferrofluid. Also, finite size effects

* Corresponding author
E-mail address: shahanegs@yahoo.com (G. Shahane)

dominate the magnetic behavior of individual nanoparticles, increasing their relevance as the particle size decreases. Quantitative understanding about the transport properties becomes important as the application of the magnetic nanofluid develops into thermal engineering. Its magnetically induced rheological effects are useful for designing magnetofluidic devices. For successfully employing of nanofluids as heat transfer fluids, these properties need to be investigated [16-18]. In this paper the authors present their results on the synthesis, characterization and rheological behavior of ferrofluid formed with oleic acid coated Fe_3O_4 nanoparticles.

2. Experimental Details

Fe_3O_4 nanoparticles of the controlled size were prepared by a facile chemical co-precipitation method. AR grade $FeCl_2$ and $FeCl_3$ were used as starting materials. For synthesis, equimolar solutions of $FeCl_2$ and $FeCl_3$ were mixed in their stoichiometric ratio and homogenized at room temperature. The pH of the solution was adjusted by adding 1M NaOH solution. Oleic acid was used as a surfactant to prevent agglomeration of particles. The mixture was then heated at 80°C for about one hour. The particles were collected at this stage by magnetic decantation method and washed several times with de-ionized water to remove unwanted residual of salts. The sample was then dried at 80°C to get fine powder and used for further characterization. For the synthesis of ferrofluid, the wet slurry was dispersed in kerosene and centrifuged at 12,000 rpm for 15 min to separate out the larger size particles.

Formation of ferrite nanoparticles by a co-precipitation method is a two-step process [13]: First conversion of metal salts into hydroxides (co-precipitation step) and second transformation of hydroxides in to nanoferrites (ferritization step). The hydroxides of metals in the form of fine particles were obtained by the co-precipitation of metal cations in alkaline medium. This is a fast process. The metal hydroxide, when heated at 80°C in an alkaline medium, is then transferred to ferrite. It requires sufficient time to convert metal hydroxides in to ferrites. The overall chemical reactions can be summarized as [19]:

$$FeCl_2 + 2FeCl_3 + 8OH^- \longrightarrow Fe(OH)_2 + 2Fe(OH)_3 \downarrow$$

$$Fe(OH)_2 + 2Fe(OH)_3 \longrightarrow Fe_3O_4 + 4H_2O$$

The samples were then characterized for structural, magnetic and rheological behavior. The X-ray diffraction (XRD) patterns of the samples were recorded on Rigaku make powder X-ray diffractometer (Model- XRG 2KW) at a scanning rate of 0.02°/s in the 2θ range from 20° to 80° at 40 kV, 30 mA with automatic divergence slit using CuKα radiation (λ=1.54059 Å). The shape, size distribution and microstructure of the samples were analyzed by using transmission electron microscope (JEOL JEM-200CX). FTIR transmission spectrum was recorded on Perkin Elmer Spectrum 65 Spectrometer from 4000 to 400 cm^{-1}. The magnetization measurements were carried out by vibrating sample magnetometer VSM Lake Shore Model 7307. The rheological properties of the samples were investigated using MCR300 Rheometer, M/s Anton Paar GmbH. A special plate-plate spindle, TG16-MRD, was employed for all the measurements. A coaxial magnetic field in perpendicular direction to the sample was applied during the rheological measurement. The measurements were performed using a constant temperature thermostatic bath (± 0.1°C). The gap between measuring plate and the sample was precisely maintained i.e. 0.3 mm with 0.3 ml of magnetic fluid.

3. Results and Discussion

The structural analysis of samples was done by powder X-ray diffraction technique using CuK_α radiation. Fig. 1 show the powder X-ray diffraction patterns for as-synthesized sample.

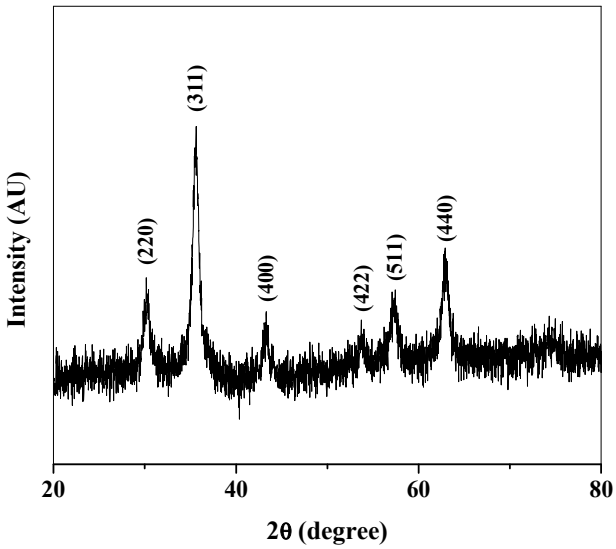

Fig. 1. XRD pattern of as-synthesized Fe_3O_4 nanoparticles.

The 'd' values and intensities of the observed diffraction peaks match with the single crystalline spinel form of Fe_3O_4 nanoparticles (JCPDS Card No. 019-0629). The discernible peaks can be indexed to (220), (311), (400), (422), (511) and (440). X-ray diffraction pattern shows broad peaks indicating ultrafine nature and small crystallite size of the particles. The lattice parameter is 8.4090 Å. The observed lattice parameter is slightly higher than the standard value indicating that samples are under strain. The strain induced in the material and the crystallite size were determined by Williamson-Hall

method; $\beta \text{ Cos } \theta = 4\varepsilon \text{ Sin } \theta + \lambda/D$ where D is the crystallite size, λ is the wavelength of the X-ray, β is full width at half maximum (FWHM) measured in radians, ε is the induced strain in system, and θ is the Bragg angle [20]. Fig. 2 shows the variation of β Cos θ versus 4 Sin θ for as-synthesized sample plotted by linear fit method. The induced strain and crystallite size were calculated from this plot and the values are 0.0027 and 11.5 nm respectively.

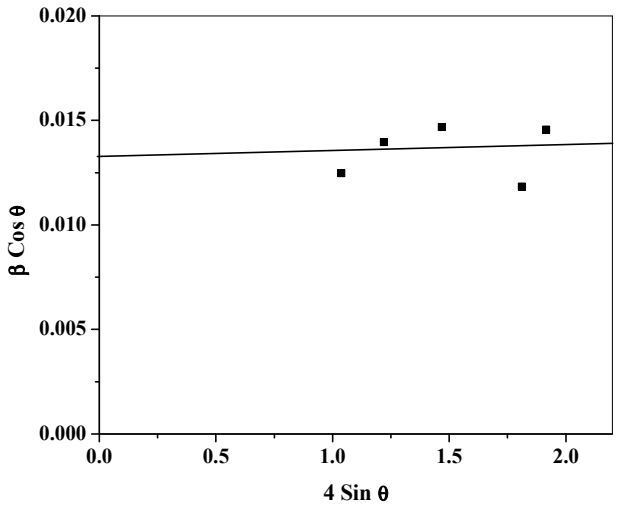

Fig. 2. Williamson-Hall plot for Fe_3O_4 nanoparticles.

The size and shape of the nanoparticles were investigated using a transmission electron microscope (TEM). Fig.3 shows a TEM image of as-synthesized Fe_3O_4 sample. The sample contains well dispersed nanoparticles of almost spherical in shape with average particle size is of the order of 10-20 nm. The TEM study supports the XRD observations.

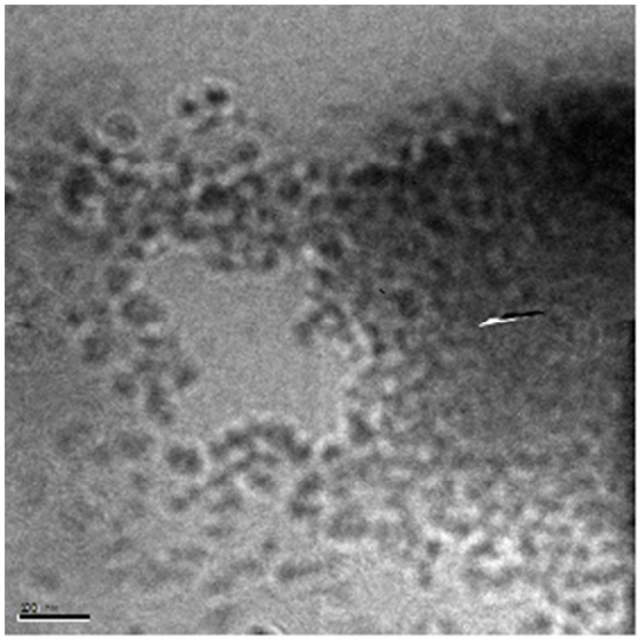

Fig. 3. TEM image of Fe_3O_4 nanoparticles.

Formation of the spinel Fe_3O_4 nanoferrite was further supported by FTIR analysis. Fig. 4 shows the FTIR spectrum of oleic acid coated Fe_3O_4 nanoparticles recorded at room temperature. Figure shows the characteristic peaks at 447cm^{-1} and 577cm^{-1} which corresponds to intrinsic stretching vibrations of the metal at the tetrahedral and octahedral sites (Fe ↔ O). Peak at 1122 cm^{-1} can be attributed to the vibrations of –CH. Peak at 1384 cm^{-1} is assigned to the vibrations of C=C in oleic acid. The strong peaks at 1636 cm^{-1} and 3404cm^{-1} can be assigned to stretching vibrations of $–CH_2$ and $–CH_3$, respectively. These all confirm that oleic acid is coated on the surface of Fe_3O_4 nanoparticles [19, 21].

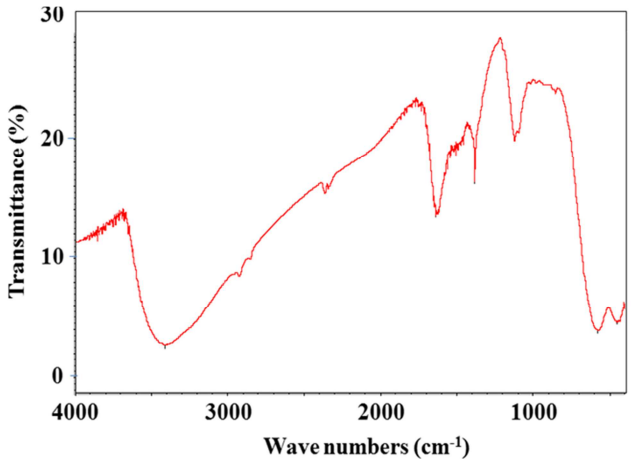

Fig. 4. FTIR spectrum of Fe_3O_4 sample.

Magnetic measurement was carried out at room temperature using vibrating sample magnetometer and Fig. 5 displays the magnetization curve for this sample. The magnetization curve demonstrates a typical superparamagnetic behavior of the as-synthesized sample. The superparamagnetism of these nanoparticles can be attributed to their fine crystallite size, which makes it easier for them to be thermally activated to overcome the magnetic anisotropy [3]. It is seen that saturation magnetism is 63emu/g and is small as compared to the bulk value. The smaller value of saturation magnetization is due to lattice defects, weaker magnetic superexchange interactions between A-sites and B-sites, and existence of a magnetically inert layer at the surface of the nanoparticles. Due their broken bonds, iron ions contained in superficial layer present a random orientation of their magnetic moments, thereby leading to a decrease of the total magnetization of each individual nanoparticle [22,23].

The magnetorheological properties were investigated on MCR300 Rheometer (M/s Anton Paar) at room temperature. Fig. 6 shows plots of the steady state shear stress in the absence/presence of the magnetic field against the shear rate. The corresponding steady state shear viscosity in the absence and in presence of the magnetic field as a function of shear rate is shown in Fig. 7.

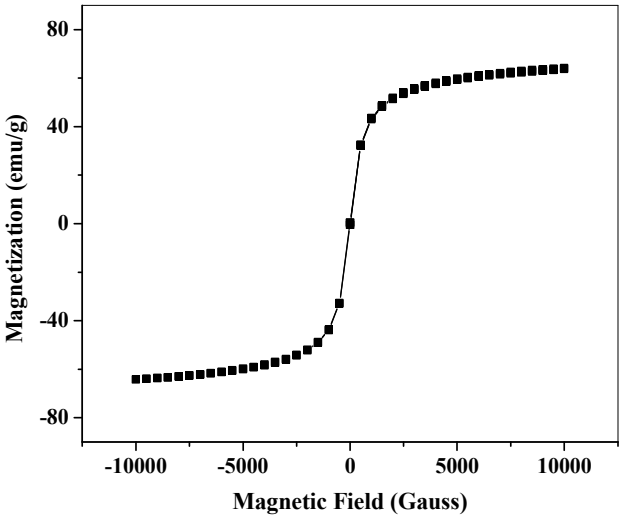

Fig. 5. Magnetization curve of Fe_3O_4 nanoparticles.

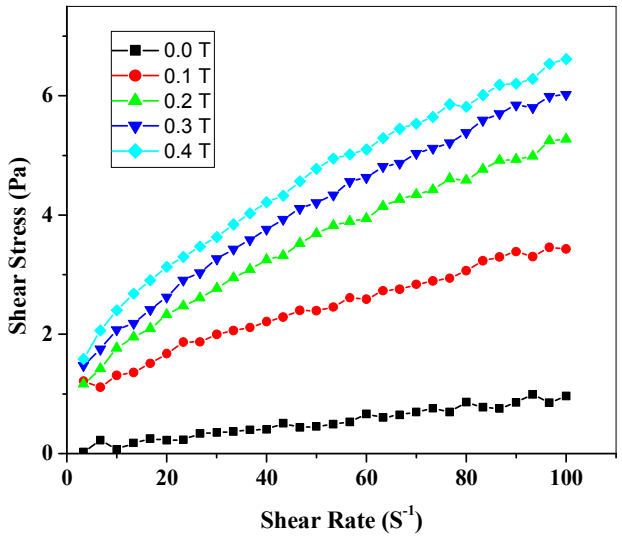

Fig. 6. Steady state shear stress against shear rate for Fe_3O_4 ferrofluid under different magnetic flux densities.

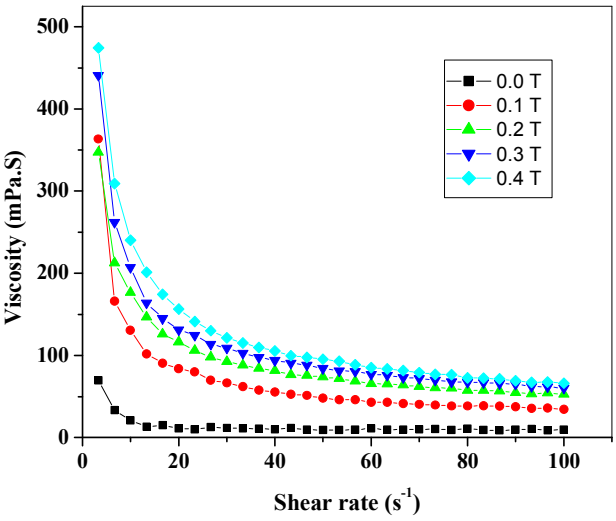

Fig. 7. Steady state viscosity against shear rate under different magnetic flux densities.

In the absence of the magnetic field, the ferrofluids behave essentially as a Newtonian fluid having a rate-insensitive viscosity because no large aggregates of the nanoparticles were formed therein. An increase in the magnetic field leads to strong changes in the viscosity. This phenomenon-the magnetoviscous effect-has been attributed to the formation of chain-like clusters due to strong interparticle interaction in the presence of a magnetic field. The hindrance of rotation of these clusters gives rise to an increase in viscosity under the influence of a magnetic field [16]. The viscosity of sample is higher at low shear rate and decreases with increasing shear rate. This shows a shear thinning behavior at the narrow limit and the Newtonian behavior for a wide range of shear rates. It is attributed to the fact that the lower shear rate is unable to break the magnetically induced structures but as the shear rate increases these structures break and fluid flows easily. Thus, the viscosity of the fluid decreases rapidly with increasing shear rate [15].

Fig. 8 shows the variation of viscosity with applied magnetic field (0–0.8 T) for the sample. This effect reveals that the formation of chain like structures is occurring as a function of magnetic field. In the system, due to the dipole-dipole interactions, the individual dipoles are arranged in a head to toe manner and tend to form a chain like structure in the direction of the force field. The dipole moment of a magnetic particle is proportional to its magnetic core volume with the relation given by $\mu=V\chi H$, where, $V=\pi d^3/6$ is the volume of the particle, d is the diameter of the particle, χ is the magnetic susceptibility of the particle and H is the applied magnetic field. With the increase of magnetic field intensity, the interaction among magnetic particles increases and hence flow resistance increases [16]. Thus viscosity of FFs increases with applied magnetic field and the fluids do not saturate even at magnetic field of 0.8 Tesla.

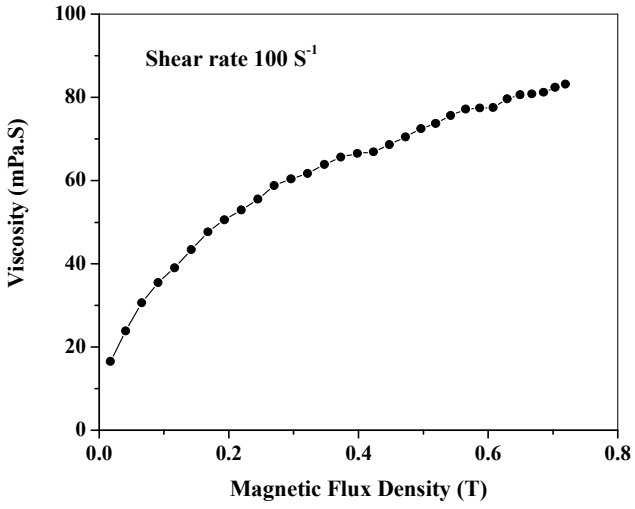

Fig. 8. Variation of viscosity with magnetic flux density.

4. Conclusion

A low temperature facile chemical co-precipitation method is used for synthesis of nanocrystalline Fe_3O_4 particles. The X-ray diffraction pattern confirms the synthesis of single crystalline phase of Fe_3O_4 nanoparticles with lattice parameter 8.4090 Å. The particle size is 11.5 nm. The introduction of the oleic acid coating did not affect the crystalline structure of Fe_3O_4 (as confirmed from X-ray diffraction) but enhanced uniform dispersion of the nanoparticles in the carrier liquid. The TEM study also confirms the nanocrystalline nature of the sample. The magnetic measurements show superparamagnetic nature of the sample with saturation magnetization 63emu/g. The ferrofluids essentially behaved as Newtonian fluids in the absence of the magnetic field, which naturally reflected the lack of large aggregates. However, under the magnetic field, the shear stress/viscosity increased because of formation of string-like clusters of nanoparticles oriented in the field direction.

Acknowledgement

One of the authors (GSS) is thankful to the Science and Engineering Research Board, Government of India, New Delhi, for the financial assistance under the Project Grant SB/S2/CMP-06/2013. Thanks are also extended to Dr. R. P. Pant, National Physical Laboratory, New Delhi for timely help and useful discussions.

References

[1] W. Brullot, N. K. Reddy, J. Wouters, V. K. Valev, B. Goderis, J. Vermant and T. Verbiest, J. Magn. Magn Mater., 324 (2012) 1919.

[2] J. P. Dery, E. F. Borra, A. M. Ritcey, Chemistry of Materials, 20 (2008) 6420.

[3] C. L. Sansom, P. Jones, R. A. Dorey, C. Beck, A. Stanhope-Bosumpim and J. Peterson, J. Magn. Magn. Mater, 335 (2013) 159.

[4] R. Patel, K. Parekh, R. V. Upadhyay and R. V. Mehta, Ind. J. Engin. & Mater. Sci., 11 (2004) 301.

[5] V. Kumar, R. P. Pant, S. K. Haldar, M. S. Yadav, Ind. J. Pure & Appl. Phys., 45 (2007) 406.

[6] O. P. Nautiyal, S. C. Bhatt, Magnetohydrodynamics, 49 (3-4) (2013) 484.

[7] S. Palacin, P. C. Hidber, J. Bourgoin, C. Miramond, C. Fermon, and G. Whitesides, Chem. Mater. 8 (1996) 1316.

[8] L. M. Yu, S. X. Cao, Y. S. Liu, J. J. Wang, J. C. Zang, J. Magn. Magn. Mater, 301 (2006) 100.

[9] J. Giri, T. Sriharsha, S. Asthana, T. K. G. Rao, A. K. Nigam and D. Bahadur, J. Magn. Magn. Mater, 293 (2005) 55.

[10] A. Rana, O. P. Thakur and Vinod Kumar, Mater. Lett, 65 (2011) 3191.

[11] K. V. P. M. Shafi, A. Gedanken, R. Prozorov, and J. Balogh, Chem. Mater.,10 (1998) 3445.

[12] D. J. Fatemi, V. G. Harris, V. M. Browning, and J. P. Kirkland, J. Appl. Phys., 83 (1998) 6867.

[13] G. S. Shahane, Ashok Kumar, M. Arora, R. P. Pant and K. Lal, J. Magn. Magn. Mater, 322 (2010) 1015.

[14] M. Chand, A. Shankar, Noorjahan, K. Jain, R. P. Pant, RSC Adv. 4 (2014) 53960.

[15] H. Shahnazian and S. Odenbach, J. Phys.: Condens. Matter, 20 (2008) 204137.

[16] K. Parekh, R. V. Upadhyay, R.V. Mehta, Hyperfine Interactions, 160 (2005) 211.

[17] M. Chand, S. Kumar, A. Shankar, R. Porwal and R. P. Pant, J. Non-Cryst. Solids, 361 (2013) 38.

[18] E. M. Rarani, N. Etesami, N. Esfahany, J. Appl. Phys., 112 (2012) 094903.

[19] S. Wu, A. Sun, F. Zhai, J. Wang, W. Xu, Q. Zhang, A. A. Volinsky, Mat. Lett, 65 (2011) 1882.

[20] A. Shankar, S. Kumar, S. Thakur, R. Porwal and R. P. Pant, Adv. Mat. Lett. 3(5) (2012) 415.

[21] J. Sun, S. Zhou, P. Hou, Y. Yang, J. Weng, X. Li, M. Li, J. Biom. Mater. Res. Part A DOI 10.1002/jbm.a (2006) 333.

[22] K. H. Wu, T. H. Ting, G.P. Wang, C. C. Yang and B.R. Mc Garvey, Mater. Res. Bull. 40 (2005) 2080.

[23] B. P. Rao, A. Maheshkumar, K. H. Rao, Y. L. N. Murthy and O. F. Caltun, J. Optoelectr. Adv. Mater. 8 (2006) 1703.